



Development of a transducer to measure instantaneous local heat flux to a surface immersed in a high temperature fluidized bed
by Jeffery Lawrence Smalley

A thesis submitted in partial fulfillment of the requirements for the degree of Master of Science in Mechanical Engineering
Montana State University
© Copyright by Jeffery Lawrence Smalley (1990)

Abstract:

The topic of this research was to develop an abrasion resistant, fast responding (approximately 2 ms) heat flux transducer to measure instantaneous local heat transfer coefficients to a surface immersed in a high temperature fluidized bed at combustion level temperatures. The principle of operation was to use eroding-type surface thermocouples in conjunction with analog circuitry to provide a d.c. output voltage that was related to the instantaneous local heat flux. A limited experimental study was performed in a high temperature fluidized bed to demonstrate that the heat flux transducer could survive the harsh environment imposed upon it and yield useful data. To the author's knowledge, there are no published values for the instantaneous local heat transfer coefficient to a horizontal cylinder immersed in a high temperature fluidized bed, therefore the accuracy of the measurements cannot be determined. However, the results obtained from the experimental study are in agreement with published values of the time average local heat transfer coefficient and the spatial average heat transfer coefficient. The data presented in this thesis are values of the instantaneous local heat transfer coefficient for a 5.08 cm diameter horizontal cylinder at the fluidized bed temperatures of 834.6 K, 821.3 K, and 1016.3 K.

**DEVELOPMENT OF A TRANSDUCER TO MEASURE
INSTANTANEOUS LOCAL HEAT FLUX TO A
SURFACE IMMERSSED IN A HIGH
TEMPERATURE FLUIDIZED BED**

by

Jeffory Lawrence Smalley

A thesis submitted in partial fulfillment
of the requirements for the degree

of

Master of Science

in

Mechanical Engineering

MONTANA STATE UNIVERSITY
Bozeman, Montana

April 1990

11378
Sm 185

APPROVAL

of a thesis submitted by

Jeffery Lawrence Smalley

This thesis has been read by each member of the thesis committee and has been found to be satisfactory regarding content, English usage, format, citations, bibliographic style, and consistency, and is ready for submission to the College of Graduate Studies.

10 April 1990
Date

Alan H. George
Chairperson, Graduate Committee

Approved for the Major Department

April 10, 1990
Date

W. E. Larsen
Head, Major Department

Approved for the College of Graduate Studies

April 11, 1990
Date

Henry J. Parsons
Graduate Dean

STATEMENT OF PERMISSION TO USE

In presenting this thesis in partial fulfillment of the requirements for a master's degree at Montana State University, I agree that the Library shall make it available to borrowers under rules of the Library. Brief quotations from this thesis are allowable without special permission, provided that accurate acknowledgment of source is made.

Permission for extensive quotation from or reproduction of this thesis may be granted by my major professor, or in his absence, by the Dean of Libraries when, in the opinion of either, the proposed use of the material is for scholarly purposes. Any copying or use of the material in this thesis for financial gain shall not be allowed without my written permission.

Signature Jeffery L. Smalley
Date 10 April 1990

ACKNOWLEDGMENTS

The author is indebted to the following persons for their contributions to this investigation:

His advisor, Dr. Alan George, for his guidance and assistance during all phases of this investigation.

Pat Vowell, for his assistance in constructing the equipment used in this investigation.

John Rompel, for constructing the special electronic equipment used in this investigation.

The staff of the Mechanical Engineering Department at Montana State University for their assistance in all aspects of this investigation.

The National Science Foundation, for their financial assistance throughout this project (grant no. CBT-8801618).

My wife Sandra Smalley, for her support during all phases of this investigation.

Rene' Tritz, for typing and checking the final version of this thesis.

TABLE OF CONTENTS

	<u>Page</u>
LIST OF TABLES	viii
LIST OF FIGURES	x
NOMENCLATURE	xv
ABSTRACT	xix
1. INTRODUCTION	1
2. DEVELOPMENT OF HEAT FLUX TRANSDUCER	6
Design of Transducer	6
Experimental Transducer	10
Test of Experimental Transducer	11
Construction of the Heat Flux Transducer	12
Materials Required	13
Tools Required	14
Construction of Thermocouples	15
Producing the Mica Sheets	16
Assembly of Transducer	16
Initial Test of Transducer	19
3. INSTRUMENTED CYLINDER	22
Introduction	22
Design of Cylinder	23
4. SIGNAL CONDITIONING CIRCUIT	26
Principle of Operation	26
Analog Signal Conditioning	28
Test of Analog Circuit	30
Contact Resistance Effects	32

TABLE OF CONTENTS—Continued

	<u>Page</u>
Adjusted Analog Circuit	35
Validation of Analog Circuit	35
5. CALIBRATION	38
Introduction	38
Analytical Solution for β	39
Experimental Values of β	41
Investigation of Calibration Results	44
Analytical Solution for k/L	46
Experimental Values of k/L	47
6. DATA ACQUISITION SYSTEM	49
Components	49
Operation	49
Data Reduction	52
7. EXPERIMENTAL RESULTS	54
Introduction	54
Test Conditions	56
Bed Material	56
Test Procedure	56
Test Results	58
Time Average Local Heat Transfer Coefficient	58
Spatial Average Heat Transfer Coefficient	64
Instantaneous Local Heat Transfer Coefficient	65
Typical Instantaneous Local Heat Transfer Coefficients in Graphical Form	66
Description of Possible Modes of Heat Transfer	82
Relative Magnitudes of the Instantaneous Heat Transfer Coefficient	87
Local Bubble Phase Heat Transfer Coefficient	89
Defective Data for Local Heat Transfer Coefficients	92

TABLE OF CONTENTS—Continued

	<u>Page</u>
8. CONCLUSIONS	93
Recommendations	94
APPENDICES	96
Appendix A—Computer Programs	97
Data Acquisition Program	98
Data Transfer Program	103
Program To Determine Superficial Gas Velocity	107
Appendix B—Fluidized Bed Facilities	109
OSU Fluidized Bed Facility	110
Test Section and Distributor Plate	111
Air Flow Measurement	112
Fuel and Temperature Controller	112
MSU Fluidized Bed Facility	113
Test Section	114
Air Supply	114
Heating Supply and Temperature Controller	114
Appendix C—Theory of Analog Circuit	116
Appendix D—RdF Gage Calibration Literature	129
REFERENCES CITED	132

LIST OF TABLES

Table	<u>Page</u>
1. Analytical Values of β at the Indicated Surface Temperature	40
2. Calibrated Values of β Obtained at the Indicated Surface Temperature	44
3. Analytical Value of k/L at the Indicated Bulk Temperature	46
4. Fluidized Bed Conditions for Each of the Test Runs Considered	57
5. Indicated Surface Temperature and Time Average Heat Transfer Coefficient for $T_{bed} = 834.6$ K, $dp = 0.9$ mm, and $U_0 = 1$ m/s	59
6. Indicated Surface Temperature and Time Average Heat Transfer Coefficient for $T_{bed} = 821.3$ K, $dp = 2.1$ mm, and $U_0 = 2.81$ m/s	59
7. Indicated Surface Temperature and Time Average Heat Transfer Coefficient for $T_{bed} = 1016.3$ K, $dp = 2.1$ mm, and $U_0 = 2.81$ m/s	60
8. Percentage of Readings Above and Below the Time Average Heat Transfer Coefficient for $T_{bed} = 834.6$ K, $dp = 0.9$ mm, and $U_0 = 1$ m/s	88
9. Percentage of Readings Above and Below the Time Average Heat Transfer Coefficient for $T_{bed} = 821.3$ K, $dp = 2.1$ mm, and $U_0 = 2.81$ m/s	88
10. Percentage of Readings Above and Below the Time Average Heat Transfer Coefficient for $T_{bed} = 1016.3$ K, $dp = 2.1$ mm, and $U_0 = 2.81$ m/s	89

LIST OF TABLES—Continued

Table	<u>Page</u>
11. Apparent Local Bubble Phase Heat Transfer Coefficient Values for $T_{bed} = 834.6$ K, $dp = 0.9$ mm, and $U_0 = 1$ m/s	90
12. Apparent Local Bubble Phase Heat Transfer Coefficient Values for $T_{bed} = 821.3$ K, $dp = 2.1$ mm, and $U_0 = 2.81$ m/s	91
13. Apparent Local Bubble Phase Heat Transfer Coefficient Values for $T_{bed} = 1016.3$ K, $dp = 2.1$ mm, and $U_0 = 2.81$ m/s	91
14. Values of the Magnitude and Angle of the Transfer Function as a Function of the Frequency	127

LIST OF FIGURES

Figure	<u>Page</u>
1. Eroding-Type Thermocouple Junction	8
2. Heat Flux Transducer for use in Instrumented Cylinder	9
3. Single Eroding-Type Thermocouple in Mounting Clamp	10
4. Resistance versus Time for First Thermocouple Test	12
5. Temperature versus Time for First Thermocouple Test	13
6. Punch used to Press Fit Thermocouple Clamp	14
7. Eroding-Type Transducer Mounted in Water Cooled Fixture	19
8. Typical Output of Heat Transfer versus Time for the MSU Fluidized Bed Test	21
9. Instrumented Cylinder	24
10. Boundary Conditions for Conduction Problem	27
11. Analog Signal Conditioning Circuit	30
12. Signal Conditioning Circuit Associated with the Heat Flux Transducer	31
13. Response of Original Signal Conditioning Circuit to a Step Change in Surface Heat Flux	32
14. Semi-Infinite Wall With Contact Resistance	33
15. Solution of the Indicated Heat Flux versus Time for Contact Resistance	34
16. Adjusted Analog Circuit	35

LIST OF FIGURES—Continued

Figure	<u>Page</u>
17. Response of Adjusted Analog Circuit to a Step Change in Surface Heat Flux	36
18. Response of Adjusted Analog Circuit to a Long Duration Step Change in Surface Heat Flux	37
19. Micro-Foil Heat Flux Transducer Used For Calibration	41
20. Schematic of Calibration Set Up	42
21. Plot of Analytical and Experimental Values of the Calibration Constant versus Ratio of Surface Temperature to Reference Temperature	45
22. Physical Model of Fluidized Bed in Operation	55
23. Angular Positions at Which Heat Flux Measurements were Made	57
24. Time Average Local Heat Transfer Coefficient versus Angular Position for $dp = 0.9$ mm, $U_0 = 1$ m/s, and $T_{bed} = 834.6$ K	61
25. Time Average Local Heat Transfer Coefficient versus Angular Position for $dp = 2.1$ mm, $U_0 = 2.81$ m/s, $T_{bed} = 821.3$ K, and $T_{bed} = 1016.3$ K	62
26. Time Average Local Heat Transfer Coefficient versus Angular Position for $dp = 2.14$ mm and $T_{bed} = 810$ K as Given by George (1984)	63
27. Time Average Local Heat Transfer Coefficient versus Angular Position for $dp = 2.14$ mm and $T_{bed} = 1052$ K as Given by George (1984)	64
28. Comparison of Present Results with Correlations of the Maximum Spatial Average Nusselt Number versus Archimedes Number	66

LIST OF FIGURES—Continued

Figure	<u>Page</u>
29. Instantaneous Local Heat Transfer Coefficient versus Time for $dp = 0.9$ mm, $\theta = 0^\circ$, $U_0 = 1$ m/s, and $T_{bed} = 834.6$ K	67
30. Instantaneous Local Heat Transfer Coefficient versus Time for $dp = 0.9$ mm, $\theta = 45^\circ$, $U_0 = 1$ m/s, and $T_{bed} = 834.6$ K	68
31. Instantaneous Local Heat Transfer Coefficient versus Time for $dp = 0.9$ mm, $\theta = 90^\circ$, $U_0 = 1$ m/s, and $T_{bed} = 834.6$ K	69
32. Instantaneous Local Heat Transfer Coefficient versus Time for $dp = 0.9$ mm, $\theta = 135^\circ$, $U_0 = 1$ m/s, and $T_{bed} = 834.6$ K	70
33. Instantaneous Local Heat Transfer Coefficient versus Time for $dp = 0.9$ mm, $\theta = 180^\circ$, $U_0 = 1$ m/s, and $T_{bed} = 834.6$ K	71
34. Instantaneous Local Heat Transfer Coefficient versus Time for $dp = 2.1$ mm, $\theta = 0^\circ$, $U_0 = 2.81$ m/s, and $T_{bed} = 821.3$ K	72
35. Instantaneous Local Heat Transfer Coefficient versus Time for $dp = 2.1$ mm, $\theta = 45^\circ$, $U_0 = 2.81$ m/s, and $T_{bed} = 821.3$ K	73
36. Instantaneous Local Heat Transfer Coefficient versus Time for $dp = 2.1$ mm, $\theta = 90^\circ$, $U_0 = 2.81$ m/s, and $T_{bed} = 821.3$ K	74
37. Instantaneous Local Heat Transfer Coefficient versus Time for $dp = 2.1$ mm, $\theta = 135^\circ$, $U_0 = 2.81$ m/s, and $T_{bed} = 821.3$ K	75

LIST OF FIGURES—Continued

Figure	<u>Page</u>
38. Instantaneous Local Heat Transfer Coefficient versus Time for $dp = 2.1$ mm, $\theta = 180^\circ$, $U_0 = 2.81$ m/s, and $T_{bed} = 821.3$ K	76
39. Instantaneous Local Heat Transfer Coefficient versus Time for $dp = 2.1$ mm, $\theta = 0^\circ$, $U_0 = 2.81$ m/s, and $T_{bed} = 1016.3$ K	77
40. Instantaneous Local Heat Transfer Coefficient versus Time for $dp = 2.1$ mm, $\theta = 45^\circ$, $U_0 = 2.81$ m/s, and $T_{bed} = 1016.3$ K	78
41. Instantaneous Local Heat Transfer Coefficient versus Time for $dp = 2.1$ mm, $\theta = 90^\circ$, $U_0 = 2.81$ m/s, and $T_{bed} = 1016.3$ K	79
42. Instantaneous Local Heat Transfer Coefficient versus Time for $dp = 2.1$ mm, $\theta = 135^\circ$, $U_0 = 2.81$ m/s, and $T_{bed} = 1016.3$ K	80
43. Instantaneous Local Heat Transfer Coefficient versus Time for $dp = 2.1$ mm, $\theta = 180^\circ$, $U_0 = 2.81$ m/s, and $T_{bed} = 1016.3$ K	81
44. 0.7 Seconds of Instantaneous Local Heat Transfer Coefficient Values at $\theta = 0^\circ$ and $T_{bed} = 834.6$ K	82
45. 0.7 Seconds of Instantaneous Local Heat Transfer Coefficient Values at $\theta = 90^\circ$ and $T_{bed} = 834.6$ K	83
46. 0.7 Seconds of Instantaneous Local Heat Transfer Coefficient Values at $\theta = 180^\circ$ and $T_{bed} = 1016.3$ K	84

LIST OF FIGURES—Continued

Figure	<u>Page</u>
47. 0.7 Seconds of Instantaneous Local Heat Transfer Coefficient Values at $\theta = 135^\circ$ and $T_{bed} = 834.6$ K	85
48. 0.7 Seconds of Instantaneous Local Heat Transfer Coefficient Values at $\theta = 45^\circ$ and $T_{bed} = 834.6$ K	86
49. 0.7 Seconds of Instantaneous Local Heat Transfer Coefficient Values at $\theta = 180^\circ$ and $T_{bed} = 834.6$ K	87
50. Data Acquisition Program	98
51. Data Transfer Program	103
52. Superficial Gas Velocity Program	107
53. Schematic of OSU High Temperature Fluidized Bed	110
54. Schematic of MSU Low Temperature Fluidized Bed	113
55. Schematic of RC-Low Pass Filter	117
56. Block Diagram of Transfer Function for the RC-Low Pass Filter	118
57. General Heat Flux Transducer	121
58. Block Diagram of Transfer Function for the RC-Low Pass Filter with Voltage Input and Output	122
59. Bode Plot for the Filter Chosen in Analog Circuit	123
60. Block Diagram of Transfer Function with Gain Amplifiers	125
61. General Circuit Diagram for Circuit that Approximates the Transfer Function	126
62. Temperature Correction Curve from the RdF Calibration Literature	131

NOMENCLATURE

ANSI	American National Standards Institute
Ar	Archimedes Number
a	thermocouple sensitivity
C	Capacitance
c	specific heat of transducer material
cm	centimeter
d.c.	direct current
db	decibels
dp	mean particle size
e	input voltage to signal conditioning circuit
f	farad
$\bar{f}(s)$	the Laplace Transform of a function, in this case $f(t)$
$G(s)$	Laplace Transform Function
g	acceleration due to gravity
hp	Hewlett Packard
Hz	Hertz
$\langle h \rangle$	time average local heat transfer coefficient
h_b	bubble phase local heat transfer coefficient
\bar{h}	spatial average local heat transfer coefficient
\bar{h}_{max}	maximum spatial average heat transfer coefficient
$h(t)$	instantaneous local heat transfer coefficient
i	current

NOMENCLATURE—Continued

j	$\sqrt{-1}$
K	degrees Kelvin
k	thermal conductivity of transducer material
k_f	thermal conductivity of fluidizing gas at bed temperature
kg	kilogram
L	effective length of transducer
m	meter
mm	millimeter
MSU	Montana State University
\overline{Nu}_{max}	maximum spatial average Nusselt Number
OSU	Oregon State University
q_{IND}	indicated heat flux with contact resistance
$q_w(t)$	instantaneous local heat flux
$\langle q_w \rangle$	time average local heat flux
$\delta q_w(t)$	instantaneous deviation of surface heat flux from time average value
$\langle q_{mf} \rangle$	average heat flux as indicated by the Micro-Foil heat flux transducer
R	resistance
R_C	contact resistance
SAE	Society of Automotive Engineers
s	Laplace transform parameter
T	temperature
T_b	bulk temperature
T_{bed}	bed temperature

NOMENCLATURE—Continued

T_L	constant temperature at $x = L$
T_W	surface temperature
$\langle T_W \rangle$	Time average surface temperature
$\delta T_W(t)$	instantaneous deviation of surface temperature from the time average value
T_1	Time average surface temperature as indicated by the first surface thermocouple
T_2	Time average surface temperature as indicated by the second surface thermocouple
T_3	Time average in-wall temperature as indicated by the in-wall thermocouple
t	time
U_0	Superficial gas velocity
V	volts
v_i	input voltage to signal conditioning circuit
v_o	output voltage from signal conditioning circuit
v_4	output voltage of signal conditioning circuit related to heat flux
W	Watts
x	position coordinate
x_1	proportionality constant between the input voltage of the signal conditioning circuit and indicated thermocouple temperature
y_1	proportionality constant between the output voltage of the signal conditioning circuit and heat flux
α	thermal diffusivity
ρ	density of transducer material
ρ_f	density of fluidizing gas at the bed temperature

NOMENCLATURE—Continued

ρ_s	density of particle
ν_f	kinematic viscosity of fluidizing gas at the bed temperature
θ	angular position on cylinder surface
μ	micro
π	constant 3.14159
ϕ	phase angle
η	dummy variable for time
ω	frequency
β	calibration constant

ABSTRACT

The topic of this research was to develop an abrasion resistant, fast responding (approximately 2 ms) heat flux transducer to measure instantaneous local heat transfer coefficients to a surface immersed in a high temperature fluidized bed at combustion level temperatures. The principle of operation was to use eroding-type surface thermocouples in conjunction with analog circuitry to provide a d.c. output voltage that was related to the instantaneous local heat flux. A limited experimental study was performed in a high temperature fluidized bed to demonstrate that the heat flux transducer could survive the harsh environment imposed upon it and yield useful data. To the author's knowledge, there are no published values for the instantaneous local heat transfer coefficient to a horizontal cylinder immersed in a high temperature fluidized bed, therefore the accuracy of the measurements cannot be determined. However, the results obtained from the experimental study are in agreement with published values of the time average local heat transfer coefficient and the spatial average heat transfer coefficient. The data presented in this thesis are values of the instantaneous local heat transfer coefficient for a 5.08 cm diameter horizontal cylinder at the fluidized bed temperatures of 834.6 K, 821.3 K, and 1016.3 K.

CHAPTER 1

INTRODUCTION

Recently a great deal of attention has been devoted to the research and development of fluidized bed combustors in the United States. There are several reasons that make fluidized beds an attractive option as opposed to using the more conventional stoker-fired and pulverized-coal-fired combustors. One of the most promising aspects of using fluidized bed combustors is improved air quality. If the bed material is composed of solid limestone or dolomite, a large portion of the sulfur dioxide released during the combustion process will be absorbed by the bed material. Furthermore, the lower temperatures characteristic of fluidized bed combustion (approximately 1123 K) tend to reduce the amount of nitrogen oxides formed during the combustion process thereby increasing air quality. Another attractive aspect of using fluidized bed combustors, according to Makansi and Schweiger (1987), is that they can be designed to burn several different types of fuels such as biomass and industrial wastes as well as coal. This means that a particular combustor may not be limited to a single type of fuel but can use whatever fuel is readily available at any particular time.

Based on information given by Makansi and Schweiger (1987) there are some drawbacks to using fluidized beds. The major drawback is that the combustion and boiler efficiency of fluidized beds are currently lower than comparably sized

pulverized-coal-fired boilers and in some cases lower than stoker-fired units. Therefore, in order to make the best use of fluidized bed combustors, it is important to understand their basic properties through research.

Many combustor designs, according to Schwieger (1985), employ arrays of horizontal tubes as heat transfer surfaces which are immersed in the fluidized bed itself. Heat transferred to the tubes is used either to generate steam or for the heating of process fluids. It is critical to have a fundamental understanding of the bed-to-surface heat transfer phenomena in high temperature fluidized beds in order to provide for accurate design and efficient operation of such systems.

Knowledge of instantaneous local heat transfer rates to surfaces immersed in low temperature fluidized beds is relatively complete. Studies involving vertical or inclined surfaces include those of Mickley et al. (1961), Tout and Clift (1973), and Gloski et al. (1984). Similar measurements for horizontal tubes have been reported by Catipovic et al. (1978, 1979, 1982). All of the above studies utilized electrically heated foils or thin metal films of low heat capacity as heat flux transducers. The operating principle of these devices, and the signal conditioning methods used, require that the transducer surface be at a higher temperature than the fluidized bed. For this reason, none of the heat flux transducers employed in the above studies are useful in high temperature fluidized beds. Despite their limitations, the above studies conducted in low temperature fluidized beds have contributed data which served to partially validate certain detailed models of the heat transfer process such as the models proposed by Adams and Welty (1979), and Decker and Glicksman (1983). However, the results obtained from these experimental studies cannot be reliably extended to the prediction of heat transfer rates to immersed surfaces in fluidized beds at combustion-level temperatures.

Time average local heat transfer coefficients for horizontal tubes immersed in high temperature fluidized beds have been reported [George and Welty (1984), Goshayeshi et al. (1985)]. While these data provide useful information concerning the local heat transfer rate around the periphery of an immersed tube, the more detailed models of the heat transfer process involve the calculation of instantaneous bed-to-surface heat transfer rates from the instantaneous flow field. These advanced analytical models cannot be validated or improved using only time average local heat transfer data.

The heat flux transducers chosen for the experiments by George and Welty (1984) and Goshayeshi et al. (1985) were thermopile type gages which use arrays of thermocouple junctions to obtain the temperature difference across thin wafers of insulating material. The problem with using this type of gage to measure the instantaneous heat transfer rate is that the gage is not abrasion resistant and must be covered with a protective film for use in fluidized beds. For use in high temperature fluidized beds, a metallic film or cover must be used. When this is done it increases the settling time of the gage. For example, Goshayeshi et al. (1985) covered a Micro-Foil heat flux gage purchased from RdF Corporation, Hudson, New Hampshire, with 0.127 mm thick stainless steel shim stock and increased the settling time from 80 ms for the gage alone to approximately 960 ms for the covered gage. The settling time referred to above is defined by Doebelin (1990), as the time, after application of a step input, for the instrument output to reach and stay within ± 5 percent of the steady state value. These values for the settling time (80 ms and 960 ms) are too long to be useful for instantaneous local heat flux measurements in fluidized beds. Therefore, in order to study instantaneous local heat transfer rates to surfaces immersed in high temperature fluidized beds, a new

heat flux transducer must be designed that can withstand the harsh environment imposed upon it.

The need for a study to measure instantaneous local heat transfer rates to surfaces immersed in high temperature fluidized beds is clear. The data are needed to validate and improve existing analytical models of the heat transfer process and for direct use in the design of immersed heat transfer surfaces. Previous attempts to accurately measure instantaneous local heat transfer rates to surfaces immersed in high temperature fluidized beds were unsuccessful due to the lack of an adequate heat flux transducer. The abrasive nature of the fluidized bed and the high temperatures involved pose significant design problems as concerns the heat flux transducer. In order to measure the instantaneous local heat flux it is necessary to develop a heat flux transducer which is abrasion resistant, capable of operation at high surface temperatures (550 K), and with sufficiently rapid response that effectively instantaneous local values of heat flux can be measured.

It was the intent of this study to develop, calibrate, and test such a heat flux transducer. There were five specific objectives in the development and testing of such a transducer:

1. To design and fabricate a heat flux transducer which was abrasion resistant, capable of operation at high temperatures, and with sufficiently rapid response that effectively instantaneous local values of the heat flux could be measured between the high temperature fluidized bed and immersed surface.
2. To design and fabricate an instrumented cylinder that contained the heat flux transducer and that could be easily mounted in the high temperature fluidized bed at Oregon State University. The work reported here was supported, in part, by the National Science Foundation under grant CBT-8801618. As part of the proposed work, it was agreed that the OSU high temperature fluidized

bed facility would be used to test the heat flux transducer and associated equipment that is the subject of this thesis. The cylinder was designed in such a fashion that the heat flux transducer was easily installed and removed from the cylinder without causing damage to either the cylinder or the transducer.

3. To design and implement a calibration scheme that determined the operational characteristics of the heat flux transducer for both steady state and transient operating conditions.
4. To program and implement a data acquisition system that interfaced with the analog signal conditioning unit which is associated with the heat flux transducer. The data acquisition system was responsible for taking time average and instantaneous temperature and heat flux readings from the analog signal conditioning unit for the heat flux transducer.
5. To prove the operation of the heat flux transducer and associated signal conditioning and data acquisition equipment by conducting a limited experimental study of instantaneous local heat transfer rates to horizontal cylinders immersed in a fluidized bed at combustion level temperatures.

CHAPTER 2

DEVELOPMENT OF THE HEAT FLUX TRANSDUCER

Design of Transducer

In the design of the heat flux transducer, several conditions had to be met. The first condition was that the transducer had to be operable at combustion level fluidized bed temperatures (approximately 1123 K). Under normal conditions the transducer will not reach a temperature this high because the instrumented cylinder, which contains the transducer, will be water cooled. However, there is a possibility that the pump controlling the water supply that cools the instrumented cylinder could fail, causing the cylinder to reach combustion level temperatures. Therefore, all materials used in the construction of the transducer can withstand temperatures up to 1123 K. Typically, however, the transducer temperature would not, in operation, exceed 550 K. Type K thermocouples, which were chosen for this application, are composed of Chromel-Alumel and have a suggested maximum operating temperature of 1533 K. This value is far greater than any expected at the OSU fluidized bed facility. Also the EMF versus temperature relationship for type K thermocouples is compatible with the circuit used in association with the heat flux transducer.

The second constraint was that the surface thermocouples had to survive in the abrasive environment caused by the solid particles in the fluidized bed. This condition was met by using thin ribbon eroding-type thermocouple junctions. Thin ribbon eroding-type thermocouple junctions of greatly different dimensions than reported here are manufactured by Nanmac Corporation, Framingham, Massachusetts. The eroding-type thermocouple junction consists of two wire ribbons pressed between three mica sheets as shown in Figure 1. The mica sheets are used as insulating material so the wire ribbons are only able to be in contact at the surface of the transducer. The actual thermocouple junction is formed by small burrs at the surface which bridge over the thin mica sheets. These burrs also contact the surface of the transducer body, creating a grounded thermocouple junction of extremely low thermal mass at the surface of the cylinder.

The next constraint that had to be met was the overall size of the heat flux transducer. The transducer was designed to fit in a 5.08 cm diameter stainless steel cylinder with a wall thickness of 0.95 cm.

The last constraint was that the heat flux transducer be easily installed and removed from the instrumented cylinder without causing damage to the cylinder or the transducer.

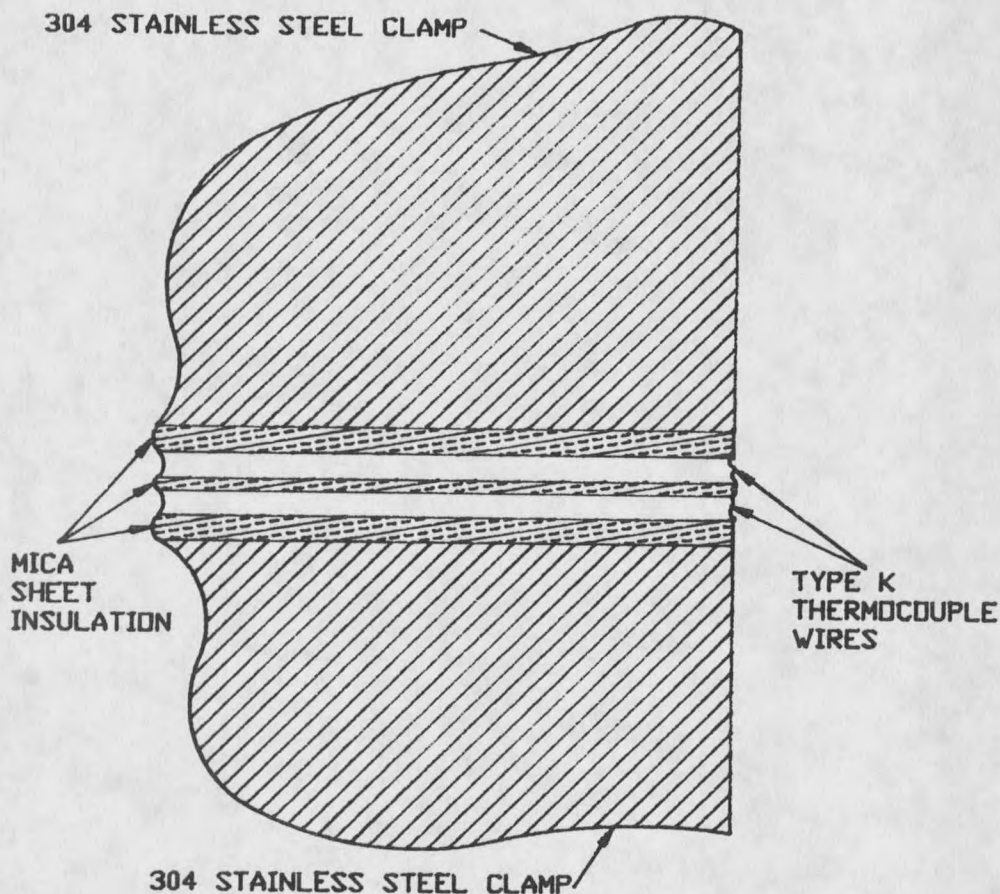


Figure 1. Eroding-Type Thermocouple Junction.

The completed design of the heat flux transducer is shown in Figure 2. The heat flux transducer, which is constructed of 304 stainless steel, contains two eroding-type thermocouples which measure the temperature at the surface of the cylinder. The transducer also contains an in-wall welded junction type K thermocouple. The welded junction thermocouple is at a depth of approximately 6 mm from the surface where the other thermocouples are positioned. The wire sleeve, which contains the thermocouple wires, has been reduced to the smallest allowable diameter so that the cooling water is not restricted at this point in the cylinder.

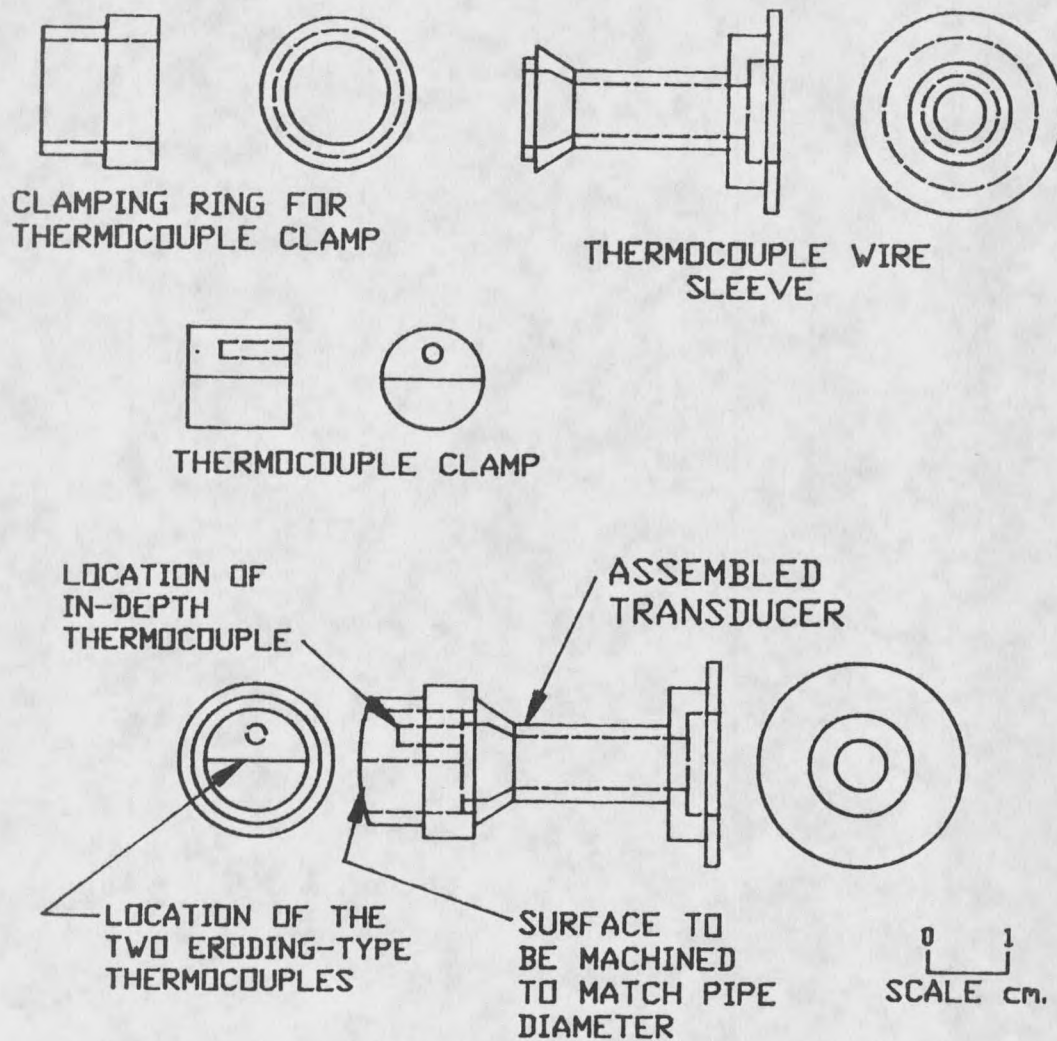


Figure 2. Heat Flux Transducer for use in Instrumented Cylinder.

It was proposed that this transducer be designed at MSU and subsequently fabricated by a vendor of specialized thermocouples. However, this was not done due to an unreasonable price relative to the project budget and long delivery time. Therefore, it was decided to build the entire heat flux transducer at MSU.

